The novel vitamin D analog ZK191784 as an intestine-specific vitamin D antagonist

Tom Nijenhuis,* Bram C. J. van der Eerden,† Ulrich Zügel,§ Andreas Steinmeyer,§ Harrie Weinans,‡ Joost G. J. Hoenderop,* Johannes P. T. M. van Leeuwen,† and René J. M. Bindels*,[1]

*Department of Physiology, Nijmegen Centre for Molecular Life Sciences, Radboud University Nijmegen Medical Centre, Nijmegen, The Netherlands; Department of †Internal Medicine and ‡Orthopedics, Erasmus Medical Centre Rotterdam, The Netherlands; and §Research Business Area Medical Chemistry, Schering AG, Berlin, Germany

ABSTRACT **Vitamin D [1,25$(OH)_2D_3$] plays a crucial role in Ca^{2+} homeostasis by stimulating Ca^{2+} (re)absorption and bone turnover. The 1,25$(OH)_2D_3$ analog ZK191784 was recently developed to dissociate the therapeutic immunomodulatory activity from the hypercalcemic side effects of 1,25$(OH)_2D_3$ and contains a structurally modified side chain characterized by a 22,23-double bond, 24R-hydroxy group, 25-cyclopropyl ring, and 5-butyloxazole unit. We investigated the effect of ZK191784 on Ca^{2+} homeostasis and the regulation of Ca^{2+} transport proteins in wild-type (WT) mice and mice lacking the renal epithelial Ca^{2+} channel TRPV5 ($TRPV5^{-/-}$). The latter display hypercalciuria, hypervitaminosis D, increased intestinal expression of the epithelial Ca^{2+} channel TRPV6, the Ca^{2+}-binding protein calbindin-D_{9K}, and intestinal Ca^{2+} hyperabsorption. ZK191784 normalized the Ca^{2+} hyperabsorption and the expression of intestinal Ca^{2+} transport proteins in $TRPV5^{-/-}$ mice. Furthermore, the compound decreased intestinal Ca^{2+} absorption in WT mice and reduced 1,25$(OH)_2D_3$-dependent $^{45}Ca^{2+}$ uptake by Caco-2 cells, substantiating a 1,25$(OH)_2D_3$-antagonistic action of ZK191784 in the intestine. ZK191784 increased renal TRPV5 and calbindin-D_{28K} expression and decreased urine Ca^{2+} excretion in WT mice. Both 1,25$(OH)_2D_3$ and ZK191784 enhanced transcellular Ca^{2+} transport in primary cultures of rabbit connecting tubules and cortical collecting ducts, indicating a 1,25$(OH)_2D_3$-agonistic effect in kidney. ZK191784 enhanced bone TRPV6 mRNA levels and 1,25$(OH)_2D_3$ as well as ZK191784 stimulated secretion of the bone formation marker osteocalcin in rat osteosarcoma cells, albeit to a different extent. In conclusion, ZK191784 is a synthetic 1,25$(OH)_2D_3$ ligand displaying a unique tissue-specific profile when administered *in vivo*. Because ZK191784 acts as an intestine-specific 1,25$(OH)_2D_3$ antagonist, this compound will be associated with less hypercalcemic side effects compared with the 1,25$(OH)_2D_3$ analogs currently used in clinical practice.—Nijenhuis, T., van der Eerden, B. C. J., Zügel, U., Steinmeyer, A., Weinans, H., Hoenderop, J. G. J., van Leeuwen, J. P. T. M., Bindels, R. J. M. The novel vitamin D analog ZK191784 as an intestine-specific vitamin D antagonist. *FASEB J.* 20, E1589–E1598 (2006)**

Key Words: TRPV5 · TRPV6 · Ca^{2+} homeostasis · 1,25$(OH)_2D_3$.

THE MAIN PHYSIOLOGICAL function of the active form of vitamin D [1,25$(OH)_2D_3$] is to stimulate intestinal and renal Ca^{2+} (re)absorption and regulate bone Ca^{2+} turnover (1, 2). In addition, 1,25$(OH)_2D_3$ has potent antiproliferative, immunosuppressive, and immunomodulatory activity (3–5). However, therapeutic administration of 1,25$(OH)_2D_3$ frequently has dose-limiting hypercalcemic side effects, increasing the risk of soft-tissue and vascular calcification as well as osteoporosis when administered in a supraphysiological dose (6, 7). Therefore, there has been great effort in identifying new 1,25$(OH)_2D_3$ analogs that retain a beneficial therapeutic profile combined with minimal calcemic action. Such analogs would have attractive clinical potential as immunomodulators in hyperproliferative disorders or to treat secondary hyperparathyroidism complicating chronic kidney disease (8).

The 1,25$(OH)_2D_3$ analog ZK191784 was developed in an effort to dissociate the immunomodulatory and hypercalcemic actions of 1,25$(OH)_2D_3$ (3). This compound contains a structurally modified side chain characterized by a 22,23-double bond, 24R-hydroxy group, 25-cyclopropyl ring, and 5-butyloxazole unit (**Fig. 1**). ZK191784 competitively binds to the vitamin D receptor (VDR) with a similar affinity as 1,25$(OH)_2D_3$ (3). Like 1,25$(OH)_2D_3$, ZK191784 inhibited antigen-induced lymphocyte proliferation and cytokine secretion *in vitro* and exhibited potent immunosuppressive activity in a murine model of contact hypersensitivity. In addition, it exerted a 1,25$(OH)_2D_3$-antagonistic effect on the promyelocytic leukemia cell line HL-60. This latter cell model is often used to study the genomic

[1]Correspondence: 286 Cell Physiology, Radboud University Nijmegen Medical Centre, P.O. Box 9101, Nijmegen, NL-6500 HB, The Netherlands. E-mail: r.bindels@ncmls.ru.nl

doi: 10.1096/fj.06-5515fje

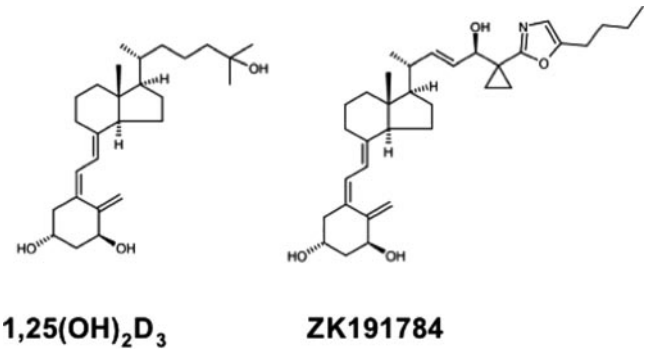

Figure 1. Chemical structure of $1,25(OH)_2D_3$ and its analog ZK191784. Compared with$1,25(OH)_2D_3$, ZK191784 contains a structurally modified side chain characterized by a 22,23-double bond, 24R-hydroxy group, 25-cyclopropyl ring and 5-butyloxazole unit.

responses of $1,25(OH)_2D_3$ analogs (3, 9), and antagonism of HL-60 differentiation was previously shown with several vitamin D analogs that have $1,25(OH)_2D_3$-antagonistic profiles *in vivo* (10–13). However, the *in vivo* effects of ZK191784 regarding Ca^{2+} homeostasis and regulation of the Ca^{2+} transport proteins have not been evaluated in detail.

$1,25(OH)_2D_3$-stimulated transcellular Ca^{2+} (re)absorption involves Ca^{2+} entry across the luminal membrane via the epithelial Ca^{2+} channels TRPV5 and TRPV6 (1, 14–16). TRPV5 is localized at the luminal membrane of the late distal convoluted tubule (DCT) and connecting tubule (CNT) in kidney. TRPV6 is the homologous epithelial Ca^{2+} channel localized along the brush-border membrane of the duodenum. After Ca^{2+} entry across the luminal membrane, Ca^{2+} bound to Ca^{2+}-binding proteins (calbindins) diffuse to the basolateral membrane of the cell. Ca^{2+} is finally extruded to the blood compartment by the Na^+/Ca^{2+} exchanger (NCX1) and/or the plasma membrane Ca^{2+}-ATPase (PMCA1b). The stimulatory effect of $1,25(OH)_2D_3$ on the expression of the epithelial Ca^{2+} channels in kidney and duodenum has been demonstrated and is probably associated with its hypercalcemic side effects (1). Furthermore, recent studies showed the expression of TRPV5 and TRPV6 in bone and demonstrated that TRPV5 is exclusively expressed in osteoclasts where it is involved in osteoclastic bone resorption (17, 18).

TRPV5 knockout ($TRPV5^{-/-}$) mice display profound renal Ca^{2+} wasting due to impaired active Ca^{2+} reabsorption in DCT and CNT (19). Furthermore, elevated serum $1,25(OH)_2D_3$ levels, intestinal Ca^{2+} hyperabsorption, and reduced bone thickness were demonstrated in these mice. We showed that additional ablation of 25-hydroxyvitamin-D_3-1α-hydroxylase (1α-OHase), the renal enzyme responsible for $1,25(OH)_2D_3$ biosynthesis, decreased intestinal TRPV6 expression and Ca^{2+} absorption in $TRPV5^{-/-}$/1α-$OHase^{-/-}$ mice (20). Therefore, hypervitaminosis D in these mice appears to represent a compensatory mechanism in an effort to counteract the significant renal Ca^{2+} leak. Thus, $TRPV5^{-/-}$ mice constitute an ideal animal model to study the effects of compounds with possible $1,25(OH)_2D_3$-antagonistic actions.

The aim of the present study was, therefore, to evaluate the *in vivo* effect of the novel $1,25(OH)_2D_3$ analog ZK191784 on Ca^{2+} and bone homeostasis in WT and $TRPV5^{-/-}$ mice. Animals were treated with ZK191784 for 28 days, after which Ca^{2+} absorption, Ca^{2+} excretion,and expression of the Ca^{2+} transport proteins in intestine, kidney, and bone was determined. In addition, bone morphometry was assessed by detailed microcomputed tomographic analysis. Further characterization of the actions of ZK191784 on intestinal, renal, and osteoblast cell lines was performed to reveal the biological profile of this novel $1,25(OH)_2D_3$ analog.

MATERIALS AND METHODS

ZK191784 treatment in $TRPV5^{+/+}$ (wild-type) and $TRPV5^{-/-}$ mice

$TRPV5^{-/-}$ mice were generated by targeted ablation of the TRPV5 gene (19). $TRPV5^{+/+}$ (wild-type) mice and $TRPV5^{-/-}$ littermates were housed in a light and temperature-controlled room with *ad libitum* access to deionized drinking water and standard pelleted chow (0.25% (wt/v) Na; 1.1% (wt/v) Ca). Ten-week-old $TRPV5^{+/+}$ and $TRPV5^{-/-}$ mice were treated during 28 days with 50 μg/kg/day ZK191784 [(5Z,7E,22E)-(1S,3R,24R)-25-(5-butyloxazole-2-yl)-26,27-cyclo-9,10-secocholesta-5,7,10(19),22-tetraene-1,3,24-triol; Schering AG, Berlin, Germany; Fig. 1; n=9] or vehicle (n=9) by daily subcutaneous injection. This dose was based on previous *in vivo* experiments using ZK191784 (3). Mice were treated for 28 days, after which the animals were housed in metabolic cages enabling ration feeding and collection of 24 h urine samples under mineral oil, preventing evaporation. At the end of the experiment the animals were killed, blood samples were taken, and duodenum, kidney, and femur were sampled. The animal ethics board of the Radboud University Nijmegen approved all animal studies.

Analytical procedures

Serum and urine Ca^{2+} concentrations were determined using a colorimetric assay as described previously (21, 22). Mouse serum PTH was measured using an immunoradiometric assay (Immutopics, San Clemente, CA). Na^+ and Li^+ concentrations were determined flame-spectrophotometrically (Eppendorf FCM 6343, Hamburg, Germany). Urine pH was measured using an electronic ion analyzer (Hanna Instruments, Szeged, Hungary).

In vivo $^{45}Ca^{2+}$ absorption assay

Intestinal Ca^{2+} absorption was assessed by measuring serum $^{45}Ca^{2+}$ at early time points after oral gavage. Mice were treated for 28 days with 50 μg/kg/day ZK191784 or vehicle as described above and were fasted 12 h before the experiment. Animals were hemodynamically stable under anesthesia during the assay. The $^{45}CaCl_2$ was administrated by oral gavage as described previously (19). Blood samples were obtained at indicated time intervals, and serum was analyzed by liquid scintillation counting. The change in the plasma Ca^{2+} con-

centration ($\Delta\mu M$) was calculated from the $^{45}Ca^{2+}$ content of the serum samples and the specific activity of the administered Ca^{2+}.

Real-time quantitative polymerase chain reaction analysis

Total RNA was extracted from duodenum, kidney, and bone using TriZol Total RNA Isolation Reagent (GIBCO, Breda, the Netherlands). Femurs, from which the bone marrow was removed by flushing with PBS, were first homogenized using a Mikro Dismembrator S (Sartorius, Goettingen, Germany). The obtained RNA was subjected to DNase treatment and reverse transcribed (22). Subsequently, the cDNA was used to determine TRPV6 and calbindin-D_{9K} mRNA levels in duodenum, TRPV5 and calbindin-D_{28K} mRNA expression in kidney, and TRPV5 and TRPV6 mRNA in bone by real-time quantitative polymerase chain reaction (PCR) as described previously (22, 23). In addition, mRNA expression of the housekeeping gene hypoxanthine-guanine phosphoribosyl transferase (HPRT) was determined as an endogenous control, which enabled calculation of specific mRNA expression levels as a ratio of HPRT. To determine the mRNA expression level of TRPV6 in human osteoblast cultures, species-specific primers and probes were used. For TRPV6, these were the forward primer, 5′-GCTTTGCTTCAGCCTTCTATATCAT-3′; reverse primer, 5′-TGGTAAGGAACAGCTCGAAGGT-3′ and 5′-AGGAGCTAGGCCACTTCTACGACTAC CCCA-3′ as probe. In the case of the housekeeping gene GAPDH, these were 5′-ATGGGGAAGGTGAAGGTCG-3′, 5′-TAAAAGCAGCCCTGGTGACC-3′, and 5′-CGCC CAATACGACCAAATCCGTTGAC-3′.

Immunohistochemistry

Staining of kidney sections for TRPV5 and calbindin-D_{28K} was performed on cryosections of periodate-lysine-paraformaldehyde fixed kidney samples as described previously (22, 23). For semiquantitative determination of protein abundance, images were made using a Zeiss fluorescence microscope equipped with a digital camera (Nikon DXM1200). Images were analyzed with the Image Pro Plus 4.1 image analysis software (Media Cybernetics, Silver Spring, MD), resulting in quantification of the protein levels as the mean of integrated optical density (IOD).

Bone analysis

To evaluate the effects of ZK191784 on bone and the possible correlation between epithelial Ca^{2+} channel expression and bone homeostasis, femurs from control and ZK191784-treated $TRPV5^{+/+}$ and $TRPV5^{-/-}$ mice were scanned using the SkyScan 1072 microtomograph (SkyScan, Antwerp, Belgium; ref 19). Scans were processed, and a three-dimensional morphometric analysis of the bone was performed, using the 3D-Calculator project free software (http://www.eur.nl/fgg/orthopaedics/Downloads.html). Measured parameters were expressed according to bone histomorphometry nomenclature (24).

$^{45}Ca^{2+}$ uptake assay in the intestinal Caco-2 cell line

We performed a $^{45}Ca^{2+}$ uptake assay in the human colon cancer Caco-2 cell line, which displays duodenal characteristics, to determine the effect of ZK191784 in an established intestinal cell model. The $^{45}Ca^{2+}$ uptake assay was performed as described previously (15). In short, confluent monolayers of Caco-2 cells were incubated for 48 h in normal Dulbecco's modified Eagle's medium (DMEM) culture medium (15) or culture medium supplemented with $1 \cdot 10^{-7}$ M $1,25(OH)_2D_3$, $1 \cdot 10^{-7}$ M ZK191784, or $1 \cdot 10^{-7}$ M $1,25(OH)_2D_3$ together with $1 \cdot 10^{-7}$ M ZK191784, respectively. Cells were washed with Krebs-Henseleit buffer (KHB) and, subsequently, were preincubated for 8 min in KHB or KHB supplemented with 10 μM of the TRPV6 blocker ruthenium red (Fluka, St. Louis, MO; ref 1). Thereafter, the preincubation buffer was exchanged for $^{45}Ca^{2+}$ uptake buffer, containing 0.1 mM $CaCl_2$, 2 mM NaH_2PO_4, 10 μM felodipine, 10 μM verapamil, and 1 μCi $^{45}CaCl_2$. After incubation for 8 min, cells were washed three times with ice-cold stop buffer consisting of KHB supplemented with 0.5 mM $CaCl_2$ and 1.5 mM $LaCl_3$. Cells were lysed in 0.1% (wt/v) SDS, and radioactivity of the lysate was measured using a liquid scintillation counter.

Transcellular Ca^{2+} transport in rabbit kidney CNT and CCD primary cell cultures

Rabbit kidney CNT and CCD tubules were immunodissected from the kidney cortex of New Zealand White rabbits and grown on permeable filters (Costar 0.33 cm^2), as described in detail previously (25). Filters containing confluent monolayers of CNT and CCD cells were incubated with normal DMEM culture medium (25) or culture medium supplemented with $1 \cdot 10^{-7}$ M $1,25(OH)_2D_3$, $1 \cdot 10^{-7}$ M ZK191784, or $1 \cdot 10^{-7}$ M $1,25(OH)_2D_3$ together with $1 \cdot 10^{-7}$ M ZK191784, respectively. After 48 h of incubation, transepithelial Ca^{2+} transport was measured during 90 min as described previously.

Osteocalcin secretion in rat osteosarcoma cells

Osteocalcin is produced by mature postproliferative osteoblasts at the onset of extracellular matrix (ECM) production. Ligand-induced osteocalcin production by reactive oxygen species (ROS) 17/2.8 cells was used to assess the bone formation potential of ZK191784. ROS 17/2.8 cells were cultured in DMEM culture medium containing 5% (v/v) charcoal treated fetal calf serum. Increasing concentrations of $1,25(OH)_2D_3$ and ZK191784 were applied for 72 h to obtain a dose-response curve. Subsequently, the amount of osteocalcin produced was measured.

Statistical analysis

Data are mean ± SE. Statistical comparisons were analyzed by one-way ANOVA and Fisher's multiple comparison. P values <0.05 were considered statistically significant. All analyses were performed using the StatView Statistical Package software (Power PC version 4.51, Berkely, CA) on an Apple iMac computer.

RESULTS

Metabolic studies in ZK191784-treated WT and $TRPV5^{-/-}$ mice

WT and $TRPV5^{-/-}$ mice were treated for 28 days with 50 μg/kg/day ZK191784 or vehicle by daily subcutaneous injection. The obtained metabolic data are shown in **Fig. 2** and **Table 1**. Genetic ablation of TRPV5 resulted in a 10-fold increase in Ca^{2+} excretion compared with WT mice (Fig. 2*A*). The *in vivo* $^{45}Ca^{2+}$ absorption measurements showed a profound enhancement of intestinal Ca^{2+} absorption in these $TRPV5^{-/-}$

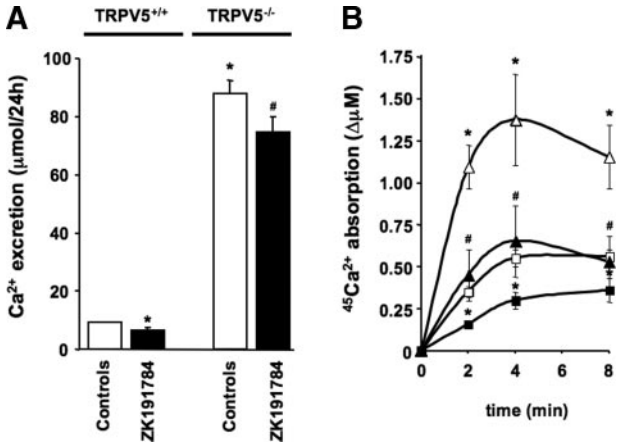

Figure 2. Renal Ca^{2+} excretion and intestinal Ca^{2+} absorption during treatment with ZK191784 in $TRPV5^{+/+}$ and $TRPV5^{-/-}$ mice. Effect of ZK191784 on renal Ca^{2+} excretion was determined in metabolic cages (*A*). Intestinal Ca^{2+} absorption was determined in an *in vivo* $^{45}Ca^{2+}$ absorption assay, measuring serum $^{45}Ca^{2+}$ at early time points after oral gavage (*B*). Controls, mice treated with vehicle only; ZK191784, mice treated for 28 days with the $1,25(OH)_2D_3$ analog ZK191784 (50 μg/kg/day). □ = $TRPV5^{+/+}$ controls, treated with vehicle only; ■ = ZK191784-treated $TRPV5^{+/+}$; △ = $TRPV5^{-/-}$ controls, treated with vehicle only; ▲ = ZK191784-treated $TRPV5^{-/-}$. Data are mean ± SE. $^*P < 0.05$ vs. $TRPV5^{+/+}$ controls; $^{\#}P < 0.05$ vs. $TRPV5^{-/-}$ controls; n = 9 animals per group.

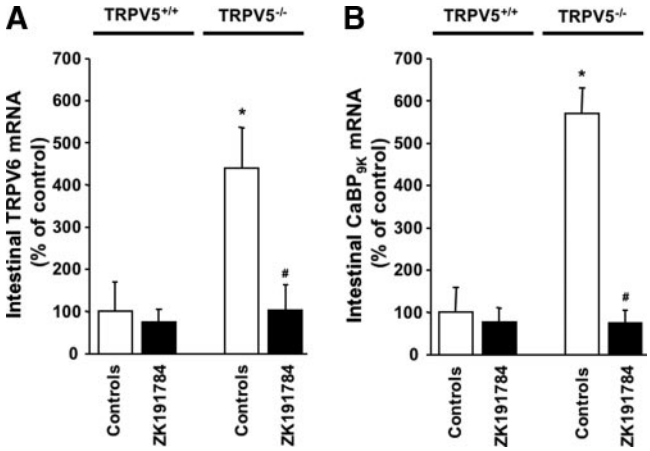

Figure 3. mRNA expression of duodenal Ca^{2+} transporters during treatment with ZK191784 in $TRPV5^{+/+}$ and $TRPV5^{-/-}$ mice. The effect of ZK191784 treatment on duodenal mRNA expression of the epithelial Ca^{2+} channel TRPV6 (*A*) and the cytosolic Ca^{2+}-binding protein calbindin-D_{9K} ($CaBP_{9K}$; *B*) was determined by real-time quantitative PCR analysis and expressed as the ratio of HPRT and depicted as percentage of $TRPV5^{+/+}$ controls. Controls, mice treated with vehicle only; ZK191784, mice treated for 28 d with the $1,25(OH)_2D_3$ analog ZK191784 (50 μg/kg/day). Data are mean ± SE. $^*P < 0.05$ vs. $TRPV5^{+/+}$ controls; $^{\#}P < 0.05$ vs. $TRPV5^{-/-}$ controls; n = 9 animals per group.

mice (Fig. 2*B*). This was accompanied by a minor but significant increase in the serum Ca^{2+} concentration (Table 1). ZK191784 treatment in $TRPV5^{-/-}$ mice normalized the intestinal Ca^{2+} hyperabsorption as well as the serum Ca^{2+} concentration. In addition, Ca^{2+} excretion was decreased by ZK191784 administration in $TRPV5^{-/-}$ mice but remained significantly elevated compared with WT mice (Fig. 2*A*). Furthermore, ZK191784 treatment significantly diminished intestinal Ca^{2+} absorption and decreased Ca^{2+} excretion in WT mice, without altering serum Ca^{2+} levels (Fig. 2*B*; Table 1). Urine volume, Na^+ excretion, and Li^+ clearance were not affected by ZK191784 in both $TRPV5^{-/-}$ and $TRPV5^{+/+}$ mice (Table 1). Furthermore, serum PTH levels did not significantly differ in the treated groups.

Duodenal mRNA expression of Ca^{2+} transport proteins

To study the effect of ZK191784 on the abundance of Ca^{2+} transporters in the intestine, TRPV6 and calbindin-D_{9K} mRNA expression was determined by real-time quantitative PCR analysis. $TRPV5^{-/-}$ mice showed profoundly increased TRPV6 (**Fig. 3*A***) and calbindin-D_{9K} (Fig. 3*B*) mRNA levels in duodenum compared with WT mice. Administration of ZK191784 to $TRPV5^{-/-}$ mice significantly reduced the TRPV6 and calbindin-D_{9K} mRNA abundance, resulting in a complete normalization of the expression of the intestinal Ca^{2+} transporters. ZK191784 treatment did not significantly alter TRPV6 and calbindin-D_{9K} mRNA levels in WT mice.

TABLE 1. *Serum and urine analysis during ZK191784 treatment in $TRPV5^{+/+}$ and $TRPV5^{-/-}$ mice*

	$TRPV5^{+/+}$		$TRPV5^{-/-}$	
	Controls	ZK191784	Controls	ZK191784
Serum				
Ca^{2+} (mM)	2.34 ± 0.02	2.36 ± 0.03	2.46 ± 0.03*	2.35 ± 0.03#
PTH (pg/ml)	11 ± 1	16 ± 5	24 ± 6	24 ± 11
Urine				
Diuresis (ml/24 h)	2.7 ± 0.1	2.1 ± 0.3	5.4 ± 0.3*	4.6 ± 0.3
Na^+ excretion (mmol/24 h)	0.1 ± 0.1	0.1 ± 0.1	0.5 ± 0.1*	0.4 ± 0.1
Li^+ clearance (μl/min)	14 ± 1	11 ± 2	16 ± 2	13 ± 1

Controls, mice treated with vehicle only; ZK191784, mice treated for 28 days with $1,25(OH)_2D_3$ analog ZK191784 (50 μg/kg/day). Data are mean ± SE. $^*P < 0.05$ vs. $TRPV5^{+/+}$ controls; $^{\#}P < 0.05$ vs. $TRPV5^{-/-}$ controls.

Renal expression of Ca^{2+} transport proteins

To evaluate the effect of ZK191784 on the expression of the Ca^{2+} transport proteins in the kidney, TRPV5 and calbindin-D_{28K} mRNA, as well as protein abundance, was determined by real-time quantitative PCR (**Fig. 4**) and semiquantitative immunohistochemistry, respectively (**Fig. 5**). ZK191784 significantly increased TRPV5 and calbindin-D_{28K} mRNA levels and enhanced protein abundance of these Ca^{2+} transporters in DCT and CNT of WT mice. In contrast, ZK191784 did not significantly alter the reduced calbindin-D_{28K} mRNA and protein expression in TRPV5$^{-/-}$ mice.

Expression of TRPV5 and TRPV6 mRNA in bone

Besides duodenum and kidney, bone is an important tissue in Ca^{2+} homeostasis and it was previously shown that the epithelial Ca^{2+} channels TRPV5 and TRPV6 are expressed in this tissue (18). Bone TRPV5 mRNA levels as determined in femur were not affected by ZK191784 in WT mice (**Fig. 6*A***). TRPV5 gene ablation did not alter the TRPV6 mRNA levels in femur (Fig. 6*B*). However, TRPV6 mRNA expression was significantly enhanced in ZK191784-treated WT and TRPV5$^{-/-}$ mice.

Bone analysis

To evaluate the effects of ZK191784 on bone morphology, femurs were scanned using microcomputed tomography (**Fig. 7**). Detailed three-dimensional morphometric analysis demonstrated that trabecular thickness (Tb.Th) is reduced in the femoral head of TRPV5$^{-/-}$ mice (**Table 2**). ZK191784 did not significantly affect the bone morphometric parameters in the femoral head of both mice strains. Analysis of the metaphysis and diaphysis showed that cortical thickness (Ct.Th) is also significantly reduced in TRPV5$^{-/-}$ mice compared with WT mice but is unaffected by ZK191784 treatment. There were no differences observed in the other trabecular and cortical bone parameters between the treated groups.

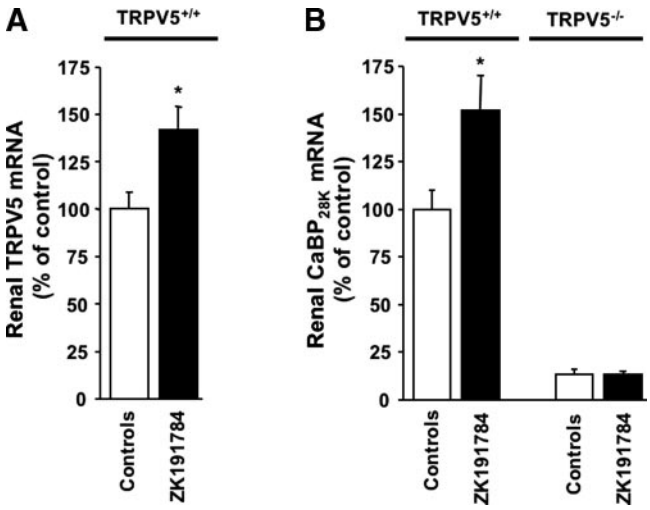

Figure 4. mRNA expression of renal Ca^{2+} transporters during treatment with ZK191784 in TRPV5$^{+/+}$ and TRPV5$^{-/-}$ mice. Effect of ZK191784 treatment on renal mRNA expression of the epithelial Ca^{2+} channel TRPV5 (*A*) and the cytosolic Ca^{2+}-binding protein calbindin-D_{28K} ($CaBP_{28K}$; *B*) was determined by real-time quantitative PCR analysis as ratio of HPRT and depicted as percentage of TRPV5$^{+/+}$ controls. Controls, mice treated with vehicle only; ZK191784, mice treated for 28 days with the $1,25(OH)_2D_3$ analog ZK191784 (50 μg/kg/day). Data are mean ± SE. *$P < 0.05$ vs. TRPV5$^{+/+}$ controls; $n = 9$ animals per group.

$^{45}Ca^{2+}$ uptake assay in the intestinal Caco-2 cell line

To determine the effect of ZK191784 in an isolated intestinal cell model, $^{45}Ca^{2+}$ uptake was determined in the human Caco-2 cell line, which has duodenal characteristics and expresses TRPV6 and calbindin-D_{9K} (1, 26). Application of $1 \cdot 10^{-7}$ M $1,25(OH)_2D_3$ for 48 h enhanced the ruthenium red-sensitive $^{45}Ca^{2+}$ uptake, substantiating the presence of $1,25(OH)_2D_3$-responsive and TRPV6-mediated Ca^{2+} absorption in these polarized epithelial intestinal cells (**Fig. 8*A***). In contrast, incubation with $1 \cdot 10^{-7}$ M ZK191784 did not stimulate $^{45}Ca^{2+}$ uptake. Importantly, concomitant application of $1 \cdot 10^{-7}$ M ZK191784 with $1 \cdot 10^{-7}$ M $1,25(OH)_2D_3$ significantly inhibited the $1,25(OH)_2D_3$-dependent $^{45}Ca^{2+}$ uptake by Caco-2 cells.

Transcellular Ca^{2+} transport in rabbit kidney CNT and CCD primary cell cultures

Transcellular Ca^{2+} transport was measured in primary cultures of immunodissected rabbit kidney CNT and CCD cells grown to confluency on permeable filter supports. Application of $1 \cdot 10^{-7}$ M $1,25(OH)_2D_3$ for 48 h enhanced transcellular Ca^{2+} absorption by the confluent monolayers (Fig. 8*B*). Importantly, $1 \cdot 10^{-7}$ M ZK191784 also stimulated Ca^{2+} transport. Addition of $1 \cdot 10^{-7}$ M $1,25(OH)_2D_3$ in the presence of $1 \cdot 10^{-7}$ M ZK191784 did not result in a further enhancement of transepithelial Ca^{2+} transport.

Osteocalcin secretion in rat osteosarcoma cells

Ligand-induced osteocalcin production by ROS 17/2.8 cells was used to assess the potential of ZK191784 to induce bone formation. Osteocalcin is produced by mature osteoblasts at the onset of ECM production. Both $1,25(OH)_2D_3$ and ZK191784 induced osteocalcin production in a dose-dependent manner (**Fig. 9**). The concentration for half maximal increase (EC_{50}) was 2.3×10^{-10} M for $1,25(OH)_2D_3$ and 5.3×10^{-8} M for ZK191784. The efficacy of ZK191784 compared with $1,25(OH)_2D_3$ was 41%.

DISCUSSION

The present study demonstrated that ZK191784 acts as an intestinal $1,25(OH)_2D_3$ antagonist by diminishing

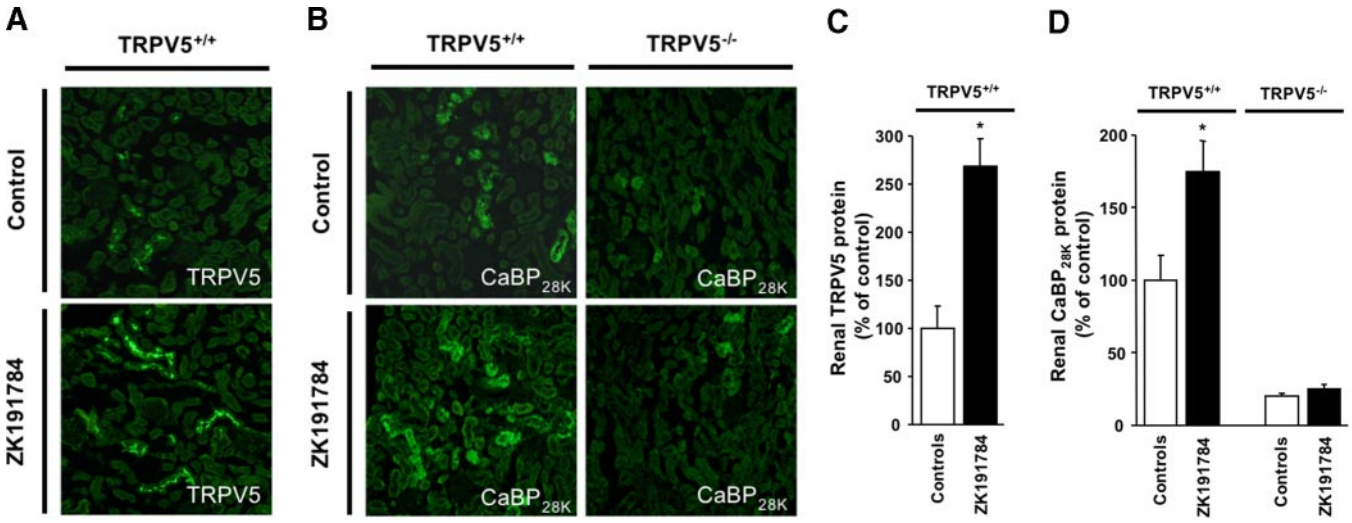

Figure 5. Protein abundance of renal Ca^{2+} transporters during treatment with ZK191784 in $TRPV5^{+/+}$ and $TRPV5^{-/-}$ mice. Representative immunohistochemical images of TRPV5 (*A*) and calbindin-D_{28K} ($CaBP_{28K}$; *B*) staining in kidney cortex. Semiquantification of renal TRPV5 (*C*) and calbindin-D_{28K} (*D*) protein abundance was performed by computerized analysis of immunohistochemical images. Data were calculated as IOD (arbitrary units) and depicted as percentage of $TRPV5^{+/+}$ controls. Controls, mice treated with vehicle only; ZK191784, mice treated for 28 d with the $1,25(OH)_2D_3$ analog ZK191784 (50 μg/kg/day). Data are mean ± SE. $^*P < 0.05$ vs. $TRPV5^{+/+}$ controls; $n = 9$ animals per group.

$1,25(OH)_2D_3$-stimulated Ca^{2+} absorption. Studies in $TRPV5^{-/-}$ mice indicated that this action was achieved by directly down-regulating intestinal Ca^{2+} transport protein expression. In contrast, *in vivo* and *in vitro* experiments indicated that ZK191784 exerts partial agonistic actions on Ca^{2+} handling in kidney. This tissue-specific partial $1,25(OH)_2D_3$ agonism/antagonism reflects a biological profile unlike any other $1,25(OH)_2D_3$ analog tested so far. Because ZK191784 does not stimulate intestinal Ca^{2+} absorption, this compound will be associated with less hypercalcemic side effects compared with$1,25(OH)_2D_3$ and its analogs currently used in clinical practice.

$1,25(OH)_2D_3$ is an important stimulatory hormone of intestinal Ca^{2+} absorption and is known to enhance the expression of the duodenal Ca^{2+} transporters (1). $TRPV5^{-/-}$ mice were previously shown to display hypervitaminosis D due to the profound renal Ca^{2+} wasting caused by abolishment of active Ca^{2+} transport in DCT and CNT (19). Indeed, these mice demonstrated significantly enhanced duodenal TRPV6 and calbindin-D_{9K} expression and Ca^{2+} hyperabsorption. Importantly, the $1,25(OH)_2D_3$ analog ZK191784 normalized the increased expression of the intestinal Ca^{2+} transporters and, thereby, antagonized intestinal Ca^{2+} hyperabsorption in $TRPV5^{-/-}$ mice. Furthermore, ZK191784 diminished Ca^{2+} absorption in WT mice. In contrast, previous studies from our laboratory demonstrated that $1,25(OH)_2D_3$ and several of its analogs enhance Ca^{2+} transporter expression and intestinal Ca^{2+} absorption in these mice (1, 27, 28). The fact that duodenal Ca^{2+} transporter expression was not significantly altered in WT mice suggests that ZK191784 might also antagonize nongenomic effects of $1,25(OH)_2D_3$ in the intestine. This finding is in line with previous studies that suggested that when dietary Ca^{2+} content is sufficient, there is only limited genomic $1,25(OH)_2D_3$-dependent stimulation of active Ca^{2+} absorption and, therefore, competitive binding of ZK191784 to the nuclear VDR does not significantly affect Ca^{2+} transporter expression in these mice (28). Taken together, these *in vivo* data indicated that ZK191784 specifically inhibits $1,25(OH)_2D_3$-stimulated intestinal Ca^{2+} absorption. To test this hypothesis *in vitro*, we used the intestine-derived Caco-2 cell line, which was previously shown to express both TRPV6 and calbindin-D_{9K} (26). These experiments showed that in the absence of $1,25(OH)_2D_3$, ZK191784 does not affect Ca^{2+} uptake by these cells. However, applied in combination with $1,25(OH)_2D_3$, ZK191784 was able to significantly diminish $1,25(OH)_2D_3$-stimulated Ca^{2+} uptake. Thus, the present data demonstrated that ZK191784, unlike $1,25(OH)_2D_3$, does not stimulate Ca^{2+} uptake by the intestine and exerts a unique antagonistic effect on $1,25(OH)_2D_3$-stimulated active Ca^{2+} absorption. This can explain why ZK191784 possesses reduced hypercalcemic potency, when administered in a dose known to exert immunosuppressive effects *in vivo* (3).

ZK191784 reduced renal Ca^{2+} excretion and significantly enhanced the expression levels of TRPV5 and calbindin-D_{28K} in WT mice. These proteins are tightly regulated by $1,25(OH)_2D_3$ and are crucial for renal Ca^{2+} reabsorption, which is exemplified by the robust hypercalciuria in $TRPV5^{-/-}$ mice (1, 19). Therefore, the concomitantly increased Ca^{2+} transporter expression and reduced Ca^{2+} excretion in WT mice suggested that ZK191784 exerts a $1,25(OH)_2D_3$-agonistic action on renal active Ca^{2+} reabsorption. The stimulatory effect of ZK191784 on transcellular Ca^{2+} transport in primary cultures of rabbit CNT and CCD substantiated these findings. Interestingly, ZK191784 did not increase

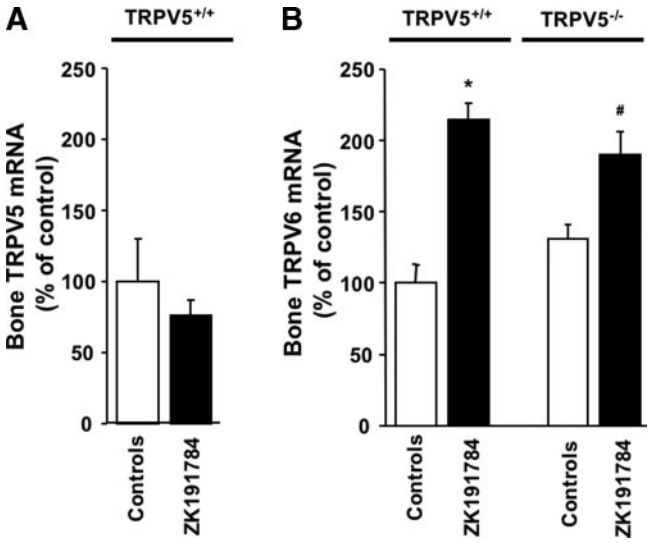

Figure 6. mRNA expression of epithelial Ca^{2+} channels in bone during treatment with ZK191784 in $TRPV5^{+/+}$ and $TRPV5^{-/-}$ mice. Effect of ZK191784 treatment on mRNA expression of the epithelial Ca^{2+} channels TRPV5 (*A*) and TRPV6 (*B*) in bone was determined by real-time quantitative PCR analysis as the ratio of HPRT and depicted as percentage of $TRPV5^{+/+}$ controls. Controls, mice treated with vehicle only; ZK191784, mice treated for 28 days with the $1,25(OH)_2D_3$ analog ZK191784 (50 μg/kg/day). Data are mean ± SE. $^*P < 0.05$ vs. $TRPV5^{+/+}$ controls; $^{\#}P < 0.05$ vs. $TRPV5^{-/-}$ controls; $n = 9$ animals per group.

calbindin-D_{28K} abundance in $TRPV5^{-/-}$ mice. However, previous studies from our group demonstrated that blockade of TRPV5-mediated Ca^{2+} influx in DCT and CNT cells down-regulates calbindin-D_{28K} expression (29). This indicated that regulation of the latter protein is highly dependent on the magnitude of the Ca^{2+} influx through TRPV5. This could explain the significantly reduced calbindin-D_{28K} expression in $TRPV5^{-/-}$ mice, despite elevated $1,25(OH)_2D_3$ levels (19), as well as the absence of a stimulatory effect of ZK191784 in these mice. Interestingly, ZK191784 still resulted in a Ca^{2+}-sparing action in $TRPV5^{-/-}$ mice that, obviously, cannot be explained by stimulation of active Ca^{2+} reabsorption. The unaffected Li^+ clearance compared with controls, as an inverse measure of proximal tubular Na^+ reabsorption to which passive Ca^{2+} reabsorption is functionally coupled, does also not support enhanced proximal tubular Ca^{2+} reabsorption. However, abolishment of the compensatory intestinal Ca^{2+} hyperabsorption and reduced serum Ca^{2+} levels will likely result in a decreased filtered Ca^{2+} load and, therefore, would be in line with the decreased Ca^{2+} excretion. Likewise, the fact that ZK191784 had only a small effect on Ca^{2+} excretion in $TRPV5^{-/-}$ mice demonstrated that the $1,25(OH)_2D_3$-mediated Ca^{2+} hyperabsorption does not contribute largely to the hypercalciuria. Together, these findings underline the presence of a primary renal Ca^{2+} leak in $TRPV5^{-/-}$ mice.

The expression of TRPV5 and TRPV6 in bone was previously demonstrated, but the functional role of these epithelial Ca^{2+} channels in this tissue remained unknown (18). In the present study, we showed that $TRPV5^{-/-}$ mice display unaltered bone TRPV6 expression, suggesting that TRPV6 does not compensate for the absence of TRPV5. This argues against redundancy of epithelial Ca^{2+} channels in bone and indicates that both channels play distinct roles in bone Ca^{2+} homeostasis. Recently, the exclusive expression of TRPV5 in the ruffled border of osteoclasts in bone was demonstrated (17). Furthermore, cultured osteoclasts from $TRPV5^{-/-}$ mice displayed reduced bone resorptive capacity, suggesting that this channel is involved in osteoclastic bone resorption. However, ZK191784 did not alter TRPV5 expression in WT mice but increased bone TRPV6 expression in both mice strains. Ligand-induced osteocalcin production by ROS 17/2.8 cells

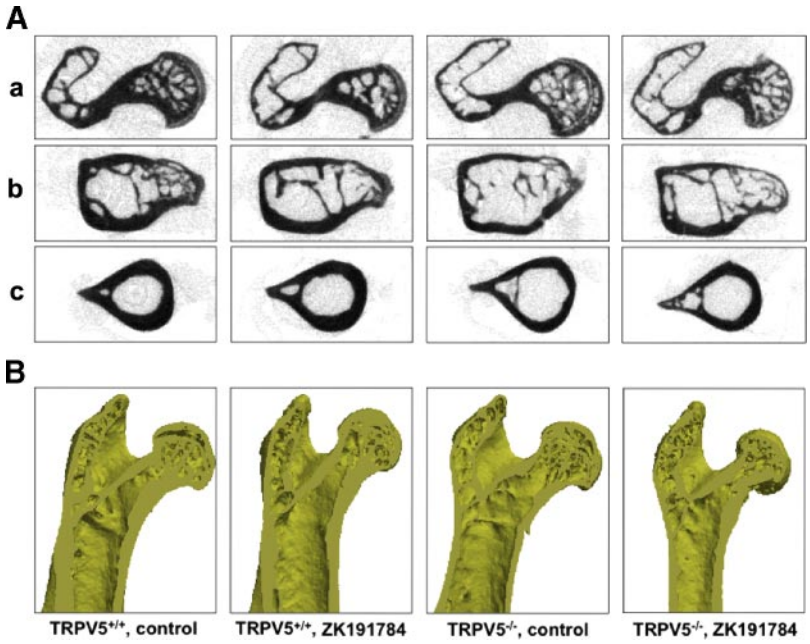

Figure 7. Bone morphometry after treatment with ZK191784 in $TRPV5^{+/+}$ and $TRPV5^{-/-}$ mice. Representative cross-sectional X-ray images of the femoral head (a), lesser trochanter (b), and diaphysis (c) in control and ZK191784-treated $TRPV5^{+/+}$ and $TRPV5^{-/-}$ mice (*A*). Three-dimensional reconstruction of femurs from control and ZK191784-treated $TRPV5^{+/+}$ and $TRPV5^{-/-}$ mice (*B*). Controls, mice treated with vehicle only; ZK191784, mice treated for 28 days with the $1,25(OH)_2D_3$ analog ZK191784 (50 μg/kg/day).

TABLE 2. *Bone analysis during ZK191784 treatment in TRPV5$^{+/+}$ and TRPV5$^{-/-}$ mice*

	TRPV5$^{+/+}$		TRPV5$^{-/-}$	
	Controls	ZK191784	Controls	ZK191784
Femoral head				
Tb.Th (μ m)	84.4 ± 2.1	82.0 ± 2.8	76.7 ± 1.1*	79.4 ± 1.8
BV/TV (%)	0.22 ± 0.01	0.21 ± 0.01	0.21 ± 0.01	0.20 ± 0.01
CD/TV (mm^{-3})	81 ± 11	112 ± 28	117 ± 15	90 ± 14
Metaphysis				
Ct.Th (μm)	299 ± 12	300 ± 7	255 ± 10*	271 ± 8†
Ct.V (mm^3)	1.9 ± 0.1	1.9 ± 0.1	1.7 ± 0.1	1.7 ± 0.1†
Ec.V (mm^3)	3.2 ± 0.1	3.4 ± 0.1	3.5 ± 0.1	3.2 ± 0.1
Dp.V (mm^3)	5.1 ± 0.2	5.3 ± 0.2	5.2 ± 0.2	4.9 ± 0.2
Ct.V/Dp.V	36.7 ± 0.5	36.3 ± 0.6	33.2 ± 0.8	34.8 ± 0.5
Diaphysis				
Ct.Th (μm)	292 ± 6	290 ± 7	247 ± 10*	256 ± 6†
Ct.V (mm^3)	1.8 ± 0.1	1.8 ± 0.1	1.7 ± 0.1	1.7 ± 0.1
Ec.V (mm^3)	3.0 ± 0.2	3.0 ± 0.1	3.1 ± 0.1	3.0 ± 0.1
Dp.V (mm^3)	4.8 ± 0.3	4.8 ± 0.1	4.8 ± 0.2	4.6 ± 0.1
Ct.V/Dp.V	36.9 ± 0.4	37.7 ± 0.4	35.9 ± 0.8	36.1 ± 0.3

Controls, mice treated with vehicle only; ZK191784, mice treated for 28 days with $1,25(OH)_2D_3$ analog ZK191784 (50 μg/kg/day). In femoral head, bone volume (BV), total bone marrow volume including trabeculae (TV), trabecular bone volume fraction (BV/TV), trabecular thickness (Tb.Th), and connectivity density (CD/TV) (measure of interconnectivity of trabecular network) were determined. In metaphysis and diaphysis, calculations were performed with regard to cortical thickness (Ct.Th), cortical volume (Ct.V), endocortical volume (Ec.V), total diaphyseal volume (Dp.V) (sum of Ct.V and Ec.V), and cortical bone volume fraction (Ct.V/Dp.V). Data are mean ± SE. *$P < 0.05$ vs. TRPV5$^{+/+}$ controls; $^{\dagger}P < 0.05$ vs. ZK191784-treated TRPV5$^{+/+}$.

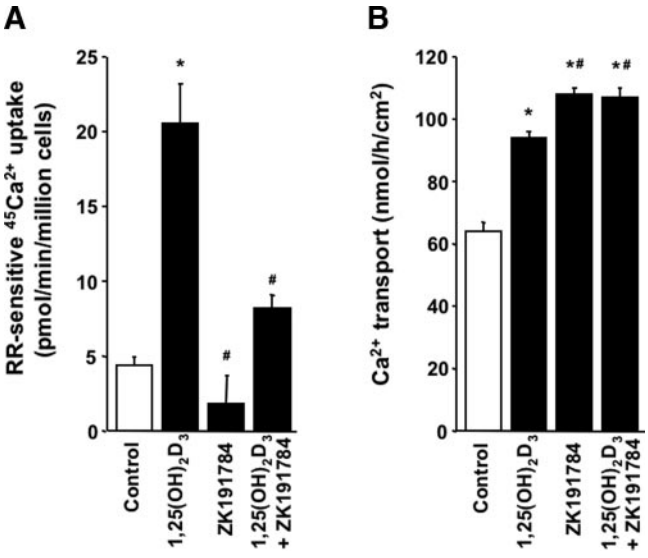

Figure 8. Differential effect of $1,25(OH)_2D_3$ and ZK191784 on $^{45}Ca^{2+}$ uptake in the intestinal Caco-2 cell line and on transepithelial Ca^{2+} transport in rabbit kidney CNT/CCD primary cell cultures. $^{45}Ca^{2+}$ uptake was determined in Caco-2 cells incubated for 48 h in normal culture medium (Control), culture medium supplemented with $1 \cdot 10^{-7}$ M $1,25(OH)_2D_3$, $1 \cdot 10^{-7}$ M ZK191784 or $1 \cdot 10^{-7}$ M $1,25(OH)_2D_3$ together with $1 \cdot 10^{-7}$ M ZK191784, respectively (*A*). Data are depicted as ruthenium red (RR)-sensitive uptake. Transcellular Ca^{2+} transport was determined in immunodissected rabbit CNT/CCD cultures incubated for 48 h in normal culture medium (Control), culture medium supplemented with $1 \cdot 10^{-7}$ M $1,25(OH)_2D_3$, $1 \cdot 10^{-7}$ M ZK191784 or $1 \cdot 10^{-7}$ M $1,25(OH)_2D_3$ together with $1 \cdot 10^{-7}$ M ZK191784 (*B*). Data are mean ± SE. *$P < 0.05$ vs. untreated cells (Control). $^{\#}P < 0.05$ vs. $1,25(OH)_2D_3$-treated cells.

was used to assess the bone formation properties of ZK191784. Although rat osteosarcoma cells secreted osteocalcin on treatment with $1,25(OH)_2D_3$ as well as ZK191784, the efficacy of the latter was rather weak. Accordingly, detailed microcomputed tomography of bone did not suggest a significantly altered bone turn-

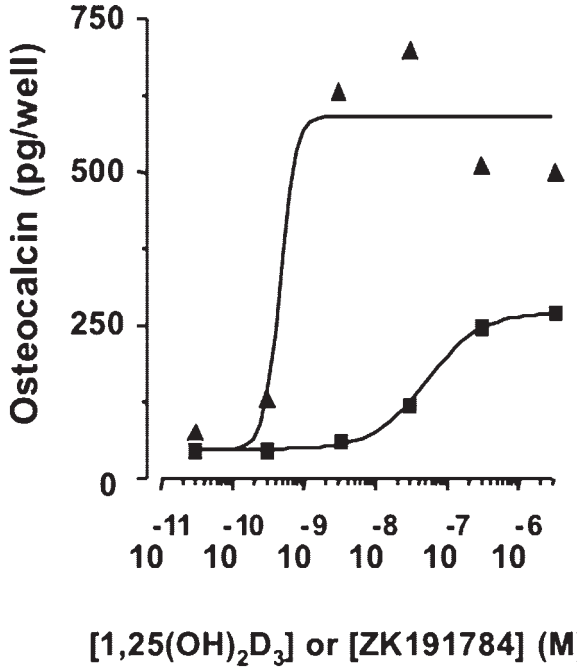

Figure 9. Effect of $1,25(OH)_2D_3$ and ZK191784 on osteocalcin production in a rat osteosarcoma cell line. Ligand-induced osteocalcin production was determined in ROS 17/2.8 cells stimulated for 72 h with increasing concentrations of $1,25(OH)_2D_3$ (▲) or ZK191784 (■) to obtain a dose-response curve (*B*).

over in ZK191784-treated mice. On the other hand, we cannot exclude that prolonged ZK191784 administration will affect bone mineral density. In addition, morphometric analysis showed that trabecular and cortical thickness was reduced in TRPV5$^{-/-}$ mice. The exact explanation for this bone phenotype remains elusive but in addition to a primary defect due to TRPV5 ablation could be a consequence of the negative Ca^{2+} balance or a direct result of the hypervitaminosis D. When administered chronically in supraphysiological concentrations, $1,25(OH)_2D_3$ was previously shown to reduce cortical bone thickness (30).

In summary, this study demonstrated that ZK191784 acts as an intestine-specific $1,25(OH)_2D_3$ antagonist. Similar tissue-specific effects have been described for *e.g.*, the partial estrogen receptor agonist tamoxifen, which was shown to exert a breast-selective, bone-sparing antagonistic action (31–34). Furthermore, our results in TRPV5$^{-/-}$ mice suggest that ZK191784 may ameliorate the clinical picture in disorders that are characterized by high $1,25(OH)_2D_3$ levels or intestinal Ca^{2+} hyperabsorption. Taken together, the unique properties of this new $1,25(OH)_2D_3$ analog might be of great benefit in clinical practice, where complete inhibition or stimulation, of the $1,25(OH)_2D_3$ endocrine system is mostly undesirable. FJ

The work was financially supported by the Dutch Kidney Foundation (C10.1881, C03.6017) and the Dutch Organization of Scientific Research (Zon-Mw 016.006.001). The authors thank the staff of the Central Animal Facility, Radboud University Nijmegen, for technical support.

REFERENCES

1. Hoenderop, J. G., Nilius, B., and Bindels, R. J. (2005) Calcium absorption across epithelia. *Physiol. Rev.* **85,** 373–422
2. Suda, T., Ueno, Y., Fujii, K., and Shinki, T. (2003) Vitamin D and bone. *J. Cell. Biochem.* **88,** 259–266
3. Zugel, U., Steinmeyer, A., Giesen, C., and Asadullah, K. (2002) A novel immunosuppressive 1α,25-dihydroxyvitamin D_3 analog with reduced hypercalcemic activity. *J. Invest. Dermatol.* **119,** 1434–1442
4. Hewison, M. (1992) Vitamin D and the immune system. *J. Endocrinol.* **132,** 173–175
5. Mathieu, C., and Adorini, L. (2002) The coming of age of 1,25-dihydroxyvitamin D_3 analogs as immunomodulatory agents. *Trends Mol. Med.* **8,** 174–179
6. Goodman, W. G., Goldin, J., Kuizon, B. D., Yoon, C., Gales, B., Sider, D., Wang, Y., Chung, J., Emerick, A., and Greaser, L., *et al.* (2000) Coronary-artery calcification in young adults with end-stage renal disease who are undergoing dialysis. *N. Engl. J. Med.* **342,** 1478–1483
7. Slatopolsky, E., and Brown, A. J. (2002) Vitamin D analogs for the treatment of secondary hyperparathyroidism. *Blood Purif.* **20,** 109–112
8. Van Leeuwen, J. P. (2005) Vitamin D: cancer and differentiation. In *Vitamin D* (Feldman, D., Pike, J. W., and Glorieux, F., eds), Elsevier Academic Press, Amsterdam, the Netherlands
9. Norman, A. W., Bishop, J. E., Bula, C. M., Olivera, C. J., Mizwicki, M. T., Zanello, L. P., Ishida, H., and Okamura, W. H. (2002) Molecular tools for study of genomic and rapid signal transduction responses initiated by $1\alpha,25(OH)_2$-vitamin D_3. *Steroids* **67,** 457–466
10. Miura, D., Manabe, K., Ozono, K., Saito, M., Gao, Q., Norman, A. W., and Ishizuka, S. (1999) Antagonistic action of novel 1α,25-dihydroxyvitamin D_3-26, 23-lactone analogs on differentiation of human leukemia cells (HL-60) induced by 1α,25-dihydroxyvitamin D_3. *J. Biol. Chem.* **274,** 16392–16399
11. Ozono, K., Saito, M., Miura, D., Michigami, T., Nakajima, S., and Ishizuka, S. (1999) Analysis of the molecular mechanism for the antagonistic action of a novel 1α,25-dihydroxyvitamin D_3 analogue toward vitamin D receptor function. *J. Biol. Chem.* **274,** 32376–32381
12. Fujishima, T., Kojima, Y., Azumaya, I., Kittaka, A., and Takayama, H. (2003) Design and synthesis of potent vitamin D receptor antagonists with A-ring modifications: remarkable effects of 2α-methyl introduction on antagonistic activity. *Bioorg. Med. Chem.* **11,** 3621–3631
13. Ji, Y., and Studzinski, G. P. (2004) Retinoblastoma protein and CCAAT/enhancer-binding protein beta are required for 1,25-dihydroxyvitamin D_3-induced monocytic differentiation of HL60 cells. *Cancer Res.* **64,** 370–377
14. Chang, Q., Hoefs, S., van der Kemp, A. W., Topala, C., Bindels, R. J., and Hoenderop, J. G. (2005) The β-glucuronidase klotho hydrolyzes and activates the TRPV5 channel. *Science* **310,** 490–493
15. Hoenderop, J. G., van der Kemp, A. W., Hartog, A., van de Graaf, S. F., van Os, C. H., Willems, P. H., and Bindels, R. J. (1999) Molecular identification of the apical Ca^{2+} channel in 1, 25-dihydroxyvitamin D_3-responsive epithelia. *J. Biol. Chem.* **274,** 8375–8378
16. Peng, J. B., Chen, X. Z., Berger, U. V., Vassilev, P. M., Tsukaguchi, H., Brown, E. M., and Hediger, M. A. (1999) Molecular cloning and characterization of a channel-like transporter mediating intestinal calcium absorption. *J. Biol. Chem.* **274,** 22739–22746
17. Van der Eerden, B. C. J., Hoenderop, J. G. J., de Vries, T. J., Schoenmaker, T., Buurman, C. J., Uitterlinden, A. G., Pols, H. A. P., Bindels, R. J. M., and van Leeuwen, J. P. T. M. (2005) The epithelial Ca^{2+} channel TRPV5 is essential for proper osteoclastic bone resorption. *Proc. Natl. Acad. Sci. U. S. A.* **102,** 17507–17512
18. Nijenhuis, T., Hoenderop, J. G., van der Kemp, A. W., and Bindels, R. J. (2003) Localization and regulation of the epithelial Ca^{2+} channel TRPV6 in the kidney. *J. Am. Soc. Nephrol.* **14,** 2731–2740
19. Hoenderop, J. G., van Leeuwen, J. P., van der Eerden, B., Kersten, F., van der Kemp, A. W., Mérrliat, A., Waarsing, E., Rossier, B., Vallon, V., and Hummler, E., *et al.* (2003) Renal Ca^{2+} wasting, hyperabsorption and reduced bone thickness in mice lacking TRPV5. *J. Clin. Invest.* **112,** 1906–1914
20. Renkema, K. Y., Nijenhuis, T., van der Eerden, B. C. J., Van der Kemp, A. W. C. M., Weinans, H., van Leeuwen, J. P., Bindels, R. J. M., and Hoenderop, J. G. J. (2005) Hypervitaminosis D mediates compensatory Ca^{2+} hyperabsorption in TRPV5 knockout mice. *J. Am. Soc. Nephrol.* **16,** 3188–3195
21. Hoenderop, J. G., Muller, D., van Der Kemp, A. W., Hartog, A., Suzuki, M., Ishibashi, K., Imai, M., Sweep, F., Willems, P. H., and van Os, C. H., *et al.* (2001) Calcitriol controls the epithelial calcium channel in kidney. *J. Am. Soc. Nephrol.* **12,** 1342–1349
22. Nijenhuis, T., Vallon, V., van der Kemp, A. W., Loffing, J., Hoenderop, J. G., and Bindels, R. J. (2005) Enhanced passive Ca^{2+} reabsorption and reduced Mg^{2+} channel abundance explains thiazide-induced hypocalciuria and hypomagnesemia. *J. Clin. Invest.* **115,** 1651–1658
23. Nijenhuis, T., Hoenderop, J. G., and Bindels, R. J. (2004) Down-regulation of Ca^{2+} and Mg^{2+} transport proteins in the kidney explains tacrolimus (FK506)-induced hypercalciuria and hypomagnesemia. *J. Am. Soc. Nephrol.* **15,** 549–557
24. Parfitt, A. M., Drezner, M. K., Glorieux, F. H., Kanis, J. A., Malluche, H., Meunier, P. J., Ott, S. M., and Recker, R. R. (1987) Bone histomorphometry: standardization of nomenclature, symbols, and units. Report of the ASBMR Histomorphometry Nomenclature Committee. *J. Bone Miner. Res.* **2,** 595–610
25. Bindels, R. J., Hartog, A., Timmermans, J., and Van Os, C. H. (1991) Active Ca^{2+} transport in primary cultures of rabbit kidney CCD: stimulation by 1,25-dihydroxyvitamin D_3 and PTH. *Am. J. Physiol.* **261,** F799–F807
26. Wood, R. J., Tchack, L., and Taparia, S. (2001) 1,25-Dihydroxyvitamin D_3 increases the expression of the CaT1 epithelial calcium channel in the Caco-2 human intestinal cell line. *BMC Physiol.* **1,** 1–11

27. Hoenderop, J. G., van der Kemp, A. W., Urben, C. M., Strugnell, S. A., and Bindels, R. J. (2004) Effects of vitamin D analogues on renal and intestinal Ca^{2+} transport proteins in 25-hydroxyvitamin D_3-1α-hydroxylase knockout mice. *Kidney Int.* **66,** 1082–1089
28. Van Cromphaut, S. J., Dewerchin, M., Hoenderop, J. G., Stockmans, I., Van Herck, E., Kato, S., Bindels, R. J., Collen, D., Carmeliet, P., and Bouillon, R., *et al.* (2001) Duodenal calcium absorption in vitamin D receptor-knockout mice: functional and molecular aspects. *Proc. Natl. Acad. Sci. U. S. A.* **98,** 13324–13329
29. Van Abel, M., Hoenderop, J. G., Friedlaender, M. M., van Leeuwen, J. P., and Bindels, R. J. (2005) Coordinated control of renal Ca^{2+} transport proteins by parathyroid hormone. *Kidney Int.* **68,** 1708–1721
30. Smith, E. A., Frankenburg, E. P., Goldstein, S. A., Koshizuka, K., Elstner, E., Said, J., Kubota, T., Uskokovic, M., and Koeffler, H. P. (2000) Effects of long-term administration of vitamin D_3 analogs to mice. *J. Endocrinol.* **165,** 163–172
31. McDonnell, D. P. (1999) The molecular pharmacology of SERMs. *Trends Endocrinol. Metab.* **10,** 301–311
32. Love, R. R., Mazess, R. B., Barden, H. S., Epstein, S., Newcomb, P. A., Jordan, V. C., Carbone, P. P., and DeMets, D. L. (1992) Effects of tamoxifen on bone mineral density in postmenopausal women with breast cancer. *N. Engl. J. Med.* **326,** 852–856
33. Love, R. R., Wiebe, D. A., Newcomb, P. A., Cameron, L., Leventhal, H., Jordan, V. C., Feyzi, J., and DeMets, D. L. (1991) Effects of tamoxifen on cardiovascular risk factors in postmenopausal women. *Ann. Intern. Med.* **115,** 860–864
34. Grese, T. A., Sluka, J. P., Bryant, H. U., Cullinan, G. J., Glasebrook, A. L., Jones, C. D., Matsumoto, K., Palkowitz, A. D., Sato, M., and Termine, J. D., *et al.* (1997) Molecular determinants of tissue selectivity in estrogen receptor modulators. *Proc. Natl. Acad. Sci. U. S. A.* **94,** 14105–14110

Received for publication November 25, 2005
Accepted for publication May 15, 2006.

The novel vitamin D analog ZK191784 as an intestine-specific vitamin D antagonist

Tom Nijenhuis,* Bram C. J. van der Eerden,† Ulrich Zügel,§ Andreas Steinmeyer,§ Harrie Weinans,‡ Joost G. J. Hoenderop,* Johannes P. T. M. van Leeuwen,† and René J. M. Bindels*,[1]

*Department of Physiology, Nijmegen Centre for Molecular Life Sciences, Radboud University Nijmegen Medical Centre, Nijmegen, The Netherlands; Department of †Internal Medicine and ‡Orthopedics, Erasmus Medical Centre Rotterdam, The Netherlands; and §Research Business Area Medical Chemistry, Schering AG, Berlin, Germany

To read the full text of this article, go to http://www.fasebj.org/cgi/doi/10.1096/fj.06-5155fje

SPECIFIC AIMS

The main physiological function of vitamin D_3 [$1,25(OH)_2D_3$] is to stimulate intestinal and renal Ca^{2+} (re)absorption and regulate bone Ca^{2+} turnover. In addition, $1,25(OH)_2D_3$ has potent antiproliferative, immunosuppressive, and immunomodulatory activity. However, therapeutic administration of $1,25(OH)_2D_3$ has dose-limiting hypercalcemic side effects. Therefore, there has been great effort in identifying new $1,25(OH)_2D_3$ analogs that retain a beneficial therapeutic profile with minimal calcemic action. The $1,25(OH)_2D_3$ analog ZK191784 was developed in an effort to dissociate the immunomodulatory and hypercalcemic actions of $1,25(OH)_2D_3$. However, the *in vivo* effects of ZK191784 regarding Ca^{2+} homeostasis have not been evaluated in detail.

$1,25(OH)_2D_3$-stimulated transcellular Ca^{2+} (re)absorption involves Ca^{2+} entry across the luminal membrane via the epithelial Ca^{2+} channels TRPV5 and TRPV6. TRPV5 is localized at the luminal membrane of the late distal convoluted tubule (DCT) and connecting tubule (CNT) in kidney. TRPV6 is the homologous epithelial Ca^{2+} channel localized along the brush-border membrane of duodenum. TRPV5 knockout ($TRPV5^{-/-}$) mice display profound renal Ca^{2+} wasting due to impaired active Ca^{2+} reabsorption in DCT and CNT. Furthermore, these mice show hypervitaminosis D leading to intestinal Ca^{2+} hyperabsorption and display reduced bone thickness.

The aim of this study was, therefore, to evaluate the effect of ZK191784 on Ca^{2+} absorption, Ca^{2+} excretion and expression of the Ca^{2+} transport proteins in intestine and kidney in wild-type (WT) and $TRPV5^{-/-}$ mice. Furthermore, the actions of ZK191784 on intestinal, renal, and osteosarcoma cell lines were characterized to reveal the biological profile of this novel $1,25(OH)_2D_3$ analog.

PRINCIPAL FINDINGS

1. Metabolic studies in ZK191784-treated WT and $TRPV5^{-/-}$ mice

WT and $TRPV5^{-/-}$ mice were treated for 28 days with 50 μg/kg/day ZK191784 or vehicle by daily subcutaneous injection. Genetic ablation of TRPV5 resulted in a 10-fold increase in Ca^{2+} excretion compared with WT mice (**Fig. 1*A***) and enhancement of intestinal Ca^{2+} absorption as determined by *in vivo* $^{45}Ca^{2+}$ absorption measurements (Fig. 1*B*), accompanied by a minor increase in the serum Ca^{2+} concentration. ZK191784 treatment in $TRPV5^{-/-}$ mice normalized the intestinal Ca^{2+} hyperabsorption as well as the serum Ca^{2+} concentration. In addition, Ca^{2+} excretion was decreased by ZK191784 administration in $TRPV5^{-/-}$ mice but remained significantly elevated compared with WT mice (Fig. 1*A*). Furthermore, ZK191784 treatment significantly diminished intestinal Ca^{2+} absorption and decreased Ca^{2+} excretion in WT mice, (Fig. 1*B*) without altering serum Ca^{2+} levels.

2. ZK191784 inhibits $1,25(OH)_2D_3$-stimulated Ca^{2+} absorption and intestinal Ca^{2+} transporter expression

To study the *in vivo* effect of ZK191784 on the abundance of Ca^{2+} transporters in the intestine, TRPV6 and calbindin-D_{9K} mRNA expression was determined by real-time quantitative polymerase chain reaction (PCR) analysis. $TRPV5^{-/-}$ mice showed profoundly increased TRPV6 and calbindin-D_{9K} mRNA levels in duodenum compared with WT mice. ZK191784 significantly reduced the TRPV6 and calbindin-D_{9K} mRNA abundance in $TRPV5^{-/-}$ mice, resulting in a complete normaliza-

[1]Correspondence: 286 Cell Physiology, Radboud University Nijmegen Medical Centre, P.O. Box 9101, Nijmegen, NL-6500 HB, The Netherlands. E-mail: r.bindels@ncmls.ru.nl

doi: 10.1096/fj.06-5515fje

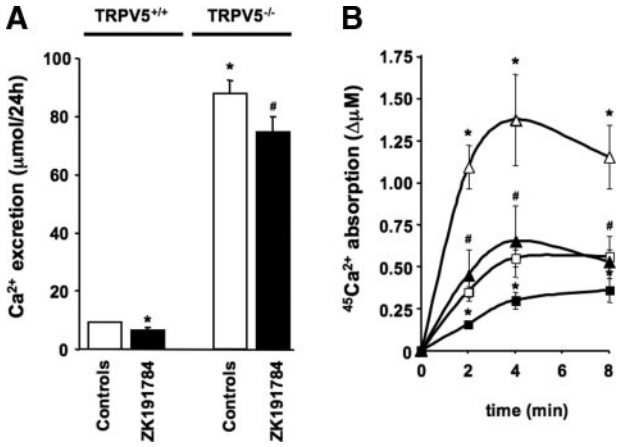

Figure 1. Renal Ca^{2+} excretion and intestinal Ca^{2+} absorption during treatment with ZK191784 in $TRPV5^{+/+}$ and $TRPV5^{-/-}$ mice. Effect of ZK191784 on renal Ca^{2+} excretion was determined in metabolic cages (*A*). Intestinal Ca^{2+} absorption was determined in an *in vivo* $^{45}Ca^{2+}$ absorption assay, measuring serum $^{45}Ca^{2+}$ at early time points after oral gavage (*B*). Controls, mice treated with vehicle only; ZK191784, mice treated for 28 days with the $1,25(OH)_2D_3$ analog ZK191784 (50 μg/kg/day). □ = $TRPV5^{+/+}$ controls, treated with vehicle only; ■ = ZK191784-treated $TRPV5^{+/+}$; △ = $TRPV5^{-/-}$ controls, treated with vehicle only; ▲ = ZK191784-treated $TRPV5^{-/-}$. Data are mean ± SE. $^*P < 0.05$ vs. $TRPV5^{+/+}$ controls; $^{\#}P < 0.05$ vs. $TRPV5^{-/-}$ controls; n = 9 animals per group.

tion of the expression of the intestinal Ca^{2+} transporters.

To determine the effect of ZK191784 in an intestinal cell model, $^{45}Ca^{2+}$ uptake was determined in the human Caco-2 cell line. Application of $1 \cdot 10^{-7}$ M $1,25(OH)_2D_3$ for 48 h enhanced the ruthenium red-sensitive $^{45}Ca^{2+}$ uptake, substantiating the presence of $1,25(OH)_2D_3$-responsive and TRPV6-mediated Ca^{2+} absorption in these polarized epithelial intestinal cells (**Fig. 2*A***). In contrast, incubation with $1 \cdot 10^{-7}$ M ZK191784 did not stimulate $^{45}Ca^{2+}$ uptake. Importantly, concomitant application of $1 \cdot 10^{-7}$ M ZK191784 and $1 \cdot 10^{-7}$ M $1,25(OH)_2D_3$ significantly inhibited the $1,25(OH)_2D_3$-dependent $^{45}Ca^{2+}$ uptake by Caco-2 cells.

3. ZK191784 up-regulates renal Ca^{2+} transport proteins and stimulates transcellular Ca^{2+} reabsorption

To evaluate the effect of ZK191784 on the expression of the Ca^{2+} transport proteins in the kidney, TRPV5 and calbindin-D_{28K} mRNA as well as protein abundance were determined by real-time quantitative PCR and semiquantitative immunohistochemistry, respectively. ZK191784 significantly increased TRPV5 and calbindin-D_{28K} mRNA levels and enhanced protein abundance of these Ca^{2+} transporters in DCT and CNT of WT mice.

Transcellular Ca^{2+} transport was measured in primary cultures of immunodissected rabbit kidney CNT and cortical collecting duct (CCD) cells grown to confluency on permeable filter supports. Application of $1 \cdot 10^{-7}$ M $1,25(OH)_2D_3$ for 48 h enhanced transcellular Ca^{2+} absorption by the confluent monolayers (Fig. 2*B*). Importantly, $1 \cdot 10^{-7}$ M ZK191784 also stimulated Ca^{2+} transport. Addition of $1 \cdot 10^{-7}$ M $1,25(OH)_2D_3$ in the presence of $1 \cdot 10^{-7}$ M ZK191784 did not result in a further enhancement of transepithelial Ca^{2+} transport.

4. Effects of ZK191784 on bone

Bone TRPV5 mRNA levels were not affected by ZK191784 in WT mice, but TRPV6 mRNA expression was significantly enhanced in ZK191784-treated WT and $TRPV5^{-/-}$ mice. Ligand-induced osteocalcin production by reactive oxygen species (ROS) 17/2.8 cells was used to assess the potential of ZK191784 to induce bone formation. Osteocalcin is produced by mature osteoblasts at the onset of extracellular matrix production. Both $1,25(OH)_2D_3$ and ZK191784 induced osteocalcin production in a dose-dependent manner.

To evaluate the *in vivo* effects of ZK191784 on bone morphology, femurs from control and ZK191784-treated mice were scanned using microcomputed tomography. Detailed three-dimensional morphometric analysis demonstrated that both trabecular and cortical

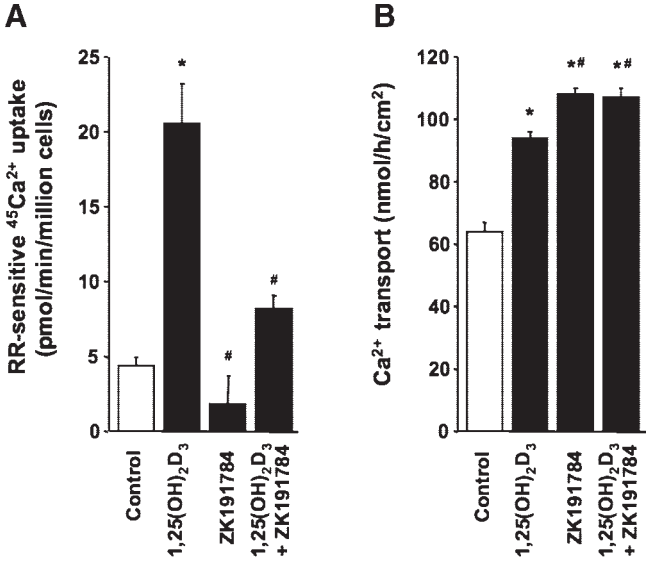

Figure 2. Differential effect of $1,25(OH)_2D_3$ and ZK191784 on $^{45}Ca^{2+}$ uptake in the intestinal Caco-2 cell line and on transepithelial Ca^{2+} transport in rabbit kidney CNT/CCD primary cell cultures. $^{45}Ca^{2+}$ uptake was determined in Caco-2 cells incubated for 48 h in normal culture medium (Control) or culture medium supplemented with $1 \cdot 10^{-7}$ M $1,25(OH)_2D_3$, $1 \cdot 10^{-7}$ M ZK191784 or $1 \cdot 10^{-7}$ M $1,25(OH)_2D_3$ together with $1 \cdot 10^{-7}$ M ZK191784, respectively (*A*). Data are depicted as ruthenium red (RR)-sensitive uptake. Transcellular Ca^{2+} transport was determined in immunodissected rabbit CNT/CCD cultures incubated for 48 h in normal culture medium (Control), culture medium supplemented with $1 \cdot 10^{-7}$ M $1,25(OH)_2D_3$, $1 \cdot 10^{-7}$ M ZK191784, or $1 \cdot 10^{-7}$ M $1,25(OH)_2D_3$ together with $1 \cdot 10^{-7}$ M ZK191784 (*B*). Data are mean ± SE. $^*P < 0.05$ vs. untreated cells (Control); $^{\#}P < 0.05$ vs. $1,25(OH)_2D_3$-treated cells.

thickness are reduced in TRPV5$^{-/-}$ mice. ZK191784 did not significantly affect bone morphometric parameters in both mice strains nor were there differences in the other trabecular and cortical bone parameters between the treated groups.

CONCLUSIONS AND SIGNIFICANCE

The present study demonstrated that ZK191784 acts as an intestinal 1,25(OH)$_2$D$_3$ antagonist by diminishing 1,25(OH)$_2$D$_3$-stimulated Ca^{2+} absorption. Studies in TRPV5$^{-/-}$ mice indicated that this action was achieved by directly down-regulating intestinal Ca^{2+} transport protein expression. In contrast, ZK191784 exerted partial agonistic actions on Ca^{2+} handling in kidney and bone. This tissue-specific partial 1,25(OH)$_2$D$_3$ agonism/antagonism reflects a biological profile unlike any other 1,25(OH)$_2$D$_3$ analog used so far (**Fig. 3**).

ZK191784 normalized the increased expression of the intestinal Ca^{2+} transporters and, thereby, antagonized the Ca^{2+} hyperabsorption in TRPV5$^{-/-}$ mice. Previous studies from our laboratory demonstrated that 1,25(OH)$_2$D$_3$ and several analogs enhance Ca^{2+} transporter expression and intestinal Ca^{2+} absorption. Furthermore, ZK191784 diminished Ca^{2+} absorption in WT mice. These data indicated that ZK191784 specifically inhibits 1,25(OH)$_2$D$_3$-stimulated intestinal Ca^{2+} absorption. To test this hypothesis *in vitro*, we used the intestine-derived Caco-2 cell line, which expresses TRPV6 and calbindin-D$_{9K}$. In the absence of 1,25(OH)$_2$D$_3$, ZK191784 did not affect Ca^{2+} uptake by these cells. However, applied in combination with 1,25(OH)$_2$D$_3$, ZK191784 was able to significantly diminish 1,25(OH)$_2$D$_3$-stimulated Ca^{2+} uptake. Thus, unlike 1,25(OH)$_2$D$_3$, ZK191784 does not stimulate Ca^{2+} uptake by the intestine and exerts a unique antagonistic effect on 1,25(OH)$_2$D$_3$-stimulated active Ca^{2+} absorption.

Renal Ca^{2+} transporter expression is tightly regulated by 1,25(OH)$_2$D$_3$. The concomitantly increased renal TRPV5 and calbindin-D$_{28K}$ expression accompanied by reduced Ca^{2+} excretion in WT mice suggested that ZK191784 exerts a 1,25(OH)$_2$D$_3$-agonistic action on renal active Ca^{2+} reabsorption. The stimulatory effect of ZK191784 on transcellular Ca^{2+} transport in primary cultures of rabbit CNT and CCD substantiated the *in vivo* findings. Interestingly, ZK191784 did not increase calbindin-D$_{28K}$ abundance in TRPV5$^{-/-}$ mice. Previous studies from our group demonstrated that calbindin-D$_{28K}$ expression is highly dependent on the TRPV5-mediated Ca^{2+} influx in DCT and CNT cells. This could explain the significantly reduced calbindin-D$_{28K}$ expression in TRPV5$^{-/-}$ mice, despite elevated 1,25(OH)$_2$D$_3$ levels, and the absence of a stimulatory effect of ZK191784 in these mice. ZK191784 still resulted in a Ca^{2+}-sparing action in TRPV5$^{-/-}$ mice that, obviously, cannot be explained by stimulation of active Ca^{2+} reabsorption. However, abolishment of Ca^{2+} hyperabsorption and reduced serum Ca^{2+} results in a decreased filtered Ca^{2+} load and, therefore, diminished Ca^{2+} excretion.

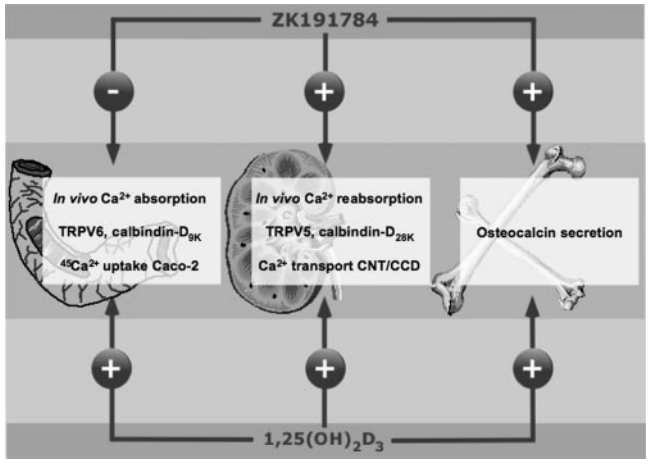

Figure 3. Schematic representation of the differential tissue-specific effects of ZK191784 compared with 1,25(OH)$_2$D$_3$ regarding Ca^{2+} homeostasis and expression of Ca^{2+} transporters. ZK191784 inhibits 1,25(OH)$_2$D$_3$-stimulated Ca^{2+} absorption *in vivo* and in the intestinal Caco-2 cell line and down-regulates 1,25(OH)$_2$D$_3$-stimulated intestinal Ca^{2+} transporter expression. ZK191784 and 1,25(OH)$_2$D$_3$ both display stimulatory effects *in vivo* on Ca^{2+} reabsorption and renal Ca^{2+} transporter expression as well as in primary cultures of immunodissected rabbit kidney CNT and CCD cells. Furthermore, ZK191784 and 1,25(OH)$_2$D$_3$ stimulate osteocalcin secretion by ROS17/2.8 cells.

The functional role of TRPV5 and TRPV6 in bone remains largely elusive. Recently, it was demonstrated that TRPV5 is exclusively expressed in the ruffled border of osteoclasts and that cultured osteoclasts from TRPV5$^{-/-}$ mice display reduced bone resorptive capacity. ZK191784 did not alter TRPV5 expression but increased bone TRPV6 expression. Ligand-induced osteocalcin production by ROS 17/2.8 cells was used to assess the bone formation properties of ZK191784. Although rat osteosarcoma cells secreted osteocalcin on treatment with 1,25(OH)$_2$D$_3$ and ZK191784, the efficacy of the latter was rather weak. Bone morphometry did not suggest altered bone turnover in ZK191784-treated mice.

In conclusion, this study demonstrated that ZK191784 is an intestine-specific 1,25(OH)$_2$D$_3$ antagonist, being one of few synthetic 1,25(OH)$_2$D$_3$ ligand displaying tissue-specific effects *in vivo*. These unique properties might be of benefit in clinical practice where complete inhibition, or stimulation, of the 1,25(OH)$_2$D$_3$ endocrine system is mostly undesirable. Our results indicate this compound will display reduced hypercalcemic potential compared with 1,25(OH)$_2$D$_3$ and its analogs currently used in clinical practice. FJ